Mendeleev Communications

Mendeleev Commun., 2025, **35**, 123–127

Two-dimensional C_6B_4 and C_8B_4 monolayers: a new family of non-classical systems with planar tetracoordinate carbon atoms and highly anisotropic mechanical properties

Stanislav A. Zaitsev,* Iliya V. Getmanskii, Tatyana N. Gribanova and Ruslan M. Minyaev

Institute of Physical and Organic Chemistry, Southern Federal University, 344090 Rostov-on-Don, Russian Federation. E-mail: stzaycev@sfedu.ru

DOI: 10.71267/mencom.7595

Crystalline forms of two-dimensional C_6B_4 and C_8B_4 monolayers designed on the basis of diboraspiropentadiene $C_3B_2H_4$ structural blocks with planar tetracoordinate carbon atoms were studied using DFT calculations. The calculations predict the structural and dynamic stability of isomeric forms of C_6B_4 and C_8B_4 monolayers, which exhibit pronounced in-plane anisotropy of mechanical properties with high values of the mechanical anisotropy coefficient (up to 6.6) and maximum values of the Poisson's ratio (up to 1.5). Isomers containing a continuous six-membered carbon ring within the structural block have negative Poisson's ratios for some directions and can be characterized as anisotropic auxetics.

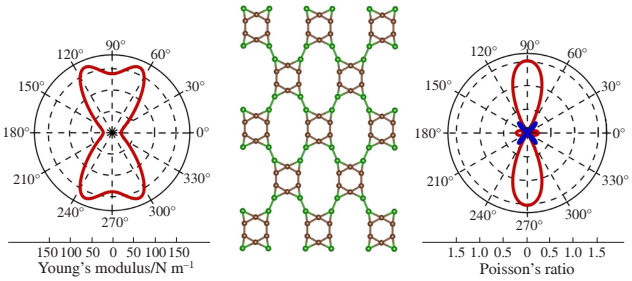

Keywords: planar tetracoordinate carbon, non-classical carbon, 2D monolayer, C_6B_4 monolayer, C_8B_4 monolayer, in-plane anisotropy, anisotropic auxetic material, mechanical anisotropy coefficient, Poisson's ratio, non-classical structural block.

The fundamental principle of the structural theory of organic compounds, which allows reliable prediction of the geometry of the vast majority of organic molecules, is the concept of the tetrahedral carbon atom **1**, proposed independently by Van't Hoff and Le Bel in 1874. A century later, a strategy for stabilizing the planar tetracoordinate carbon (ptC) center **2** was proposed,[1] challenging theorists and experimentalists and initiating numerous studies in this area.[2–4] The principles of ptC stabilization, including electronic (σ-donor and π-acceptor substituents, aromaticity of the system) and steric (rigid structural framework, correspondence between the sizes of the framework and the included atom) factors, as well as their combinations, were confirmed by the discovery of a number of organoelement and organometallic compounds with planar carbon.[2–10]

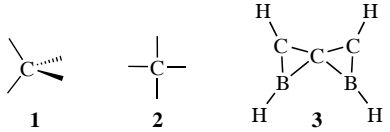

1 **2** **3**

The next step in this direction is to study graphene-like 2D surfaces formed on the basis of ptC structural blocks,[11–17] but examples of such systems are still few. As theoretical studies predict,[11–17] the unusual geometric structure determines the unusual properties of such systems (superconductivity, electronic and mechanical anisotropy, *etc.*), which makes non-classical systems promising candidates for the design of next-generation materials,[11] and the search for suitable structural blocks for constructing such systems is one of the pressing problems of modern chemistry.

The simplest example of an organoboron system with ptC is the previously proposed diboraspiropentene $C_3B_2H_4$ molecule,[18] the most stable isomer of which is represented by structure **3**. As subsequent studies have shown,[19–25] it can be an extremely convenient building block for the formation of a wide variety of derivatives, such as systems with an extended framework **4**,[20] crown-type derivatives **5**,[23] metal complexes **6**,[23] tubular systems **7**,[21] chain forms **8**[21,24] and oligomeric derivatives **9**.[25] However, 2D surfaces based on the diboraspiropentadiene building block have not yet been studied.

In this work, we studied for the first time the structure, stability and properties of a new family of 2D surfaces based on diboraspiropentadiene **3**. The approach we propose is based on the use of dimerized building blocks **10** for the formation of crystalline systems. Compared with monomer **3**, dimerized building blocks **10** are characterized by a more rigid framework and higher symmetry, which facilitates the delocalization of π-electron in the composite system and contributes to the stability of crystalline planar forms. We considered two types of isomeric systems, one pair **10a**,**b** of which is constructed from dimerized structural blocks, and the second pair **11a**,**b** includes additional >C–C< bridges inside the structural block. The calculation procedure is described in Online Supplementary Materials.

As calculations have shown, structural blocks **10** and **11** make it possible to form various types of crystalline surfaces. In this work, we investigated four types of planar structures that have a base-centered orthorhombic Bravais crystal lattice with the parameters presented in Table 1. In all cases, carbon and boron atoms form a perfectly flat sheet of monatomic thickness with many ptC centers.

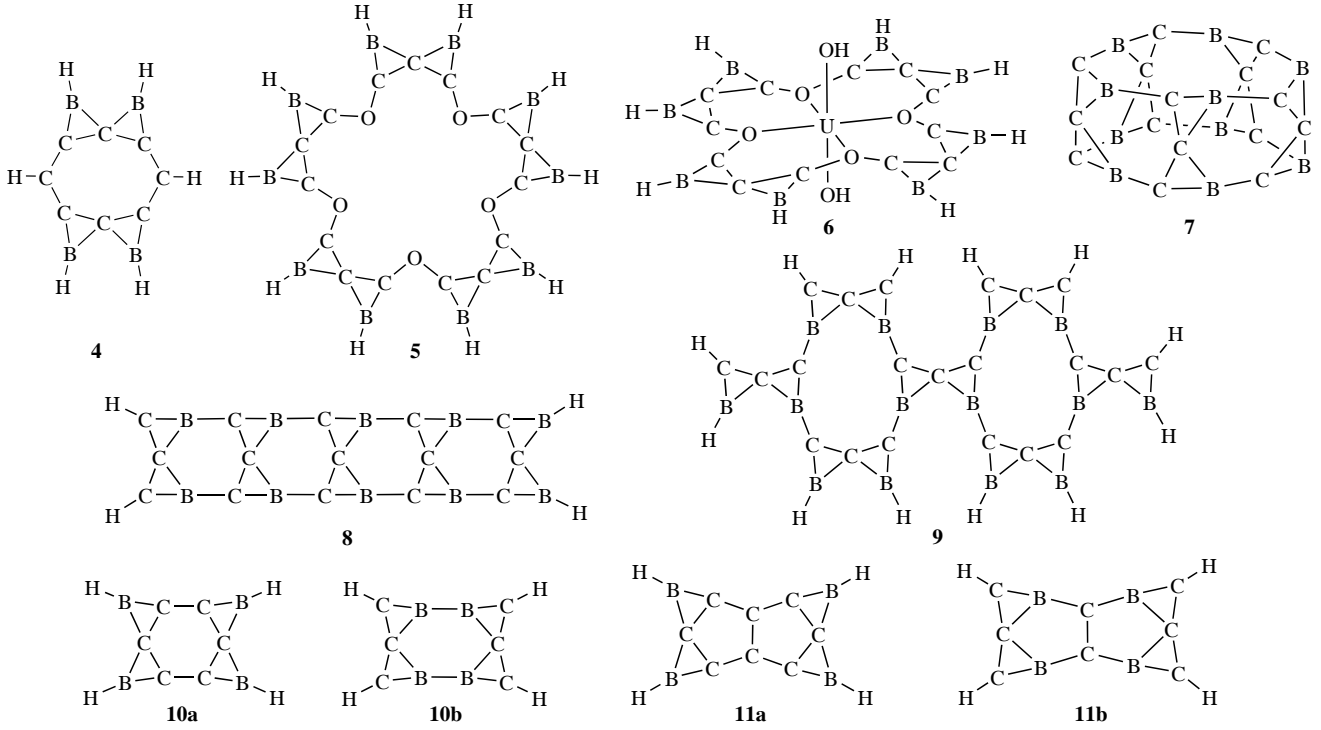

Table 1 Calculated lattice constants a and b, surface density ρ_{2D} and specific surface area (SSA) for 2D monolayers.

System	a/Å	b/Å	ρ_{2D}/mg m^{-2}	SSA/m^2 g^{-1}
oc-*ex*-C_6B_4	7.072	11.428	0.474	4221
oc-*in*-C_6B_4	7.033	11.331	0.481	4162
oc-*ex*-C_8B_4	7.660	13.694	0.441	4534
oc-*in*-C_8B_4	7.242	13.817	0.462	4325

Based on building blocks **10a**,**b**, two isomeric crystalline forms can be formed (Figure 1). The basis of the Bravais lattice in the case of the primitive unit cell consists of six carbon and four boron atoms in a stoichiometric ratio of 6 : 4 (C_6B_4). The calculated ptC–B interatomic distances in oc-*ex*-C_6B_4 and oc-*in*-C_6B_4 crystals are 1.605 and 1.612 Å, respectively, and are slightly elongated compared to the single C–B bonds (1.56 Å).[26] The calculated ptC–C interatomic distances in these crystals are 1.439 and 1.415 Å, respectively, which corresponds to intermediate values between single (1.54 Å)[26] and double (1.34 Å)[26] bonds and are characteristic of aromatic compounds.

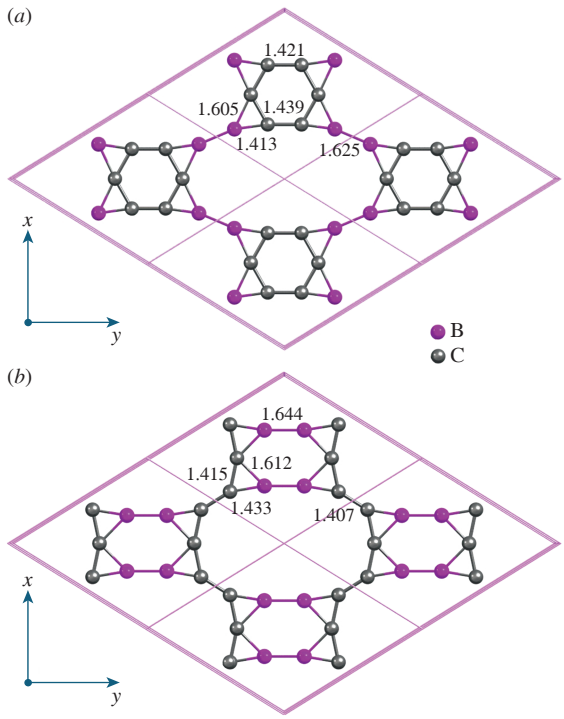

Figure 1 Geometric characteristics of (*a*) oc-*ex*-C_6B_4 and (*b*) oc-*in*-C_6B_4 2D crystals.

To evaluate the stability of the C_6B_4 monolayers, their cohesive energy (E_{coh}) was computed, which is a generally accepted descriptor for assessing the bonding strength of connected frameworks and the feasibility of experimental implementation for the predicted 2D material. The computed cohesive energies for the oc-*ex*-C_6B_4 and oc-*in*-C_6B_4 monolayers are 6.64 and 6.71 eV per atom, respectively, significantly inferior to graphene (10.13 eV per atom[27]), but superior to the characteristics of 2D carborane (5.92 eV per atom[28]), silicene (4.57 eV per atom[29]) and germanene (3.74 eV per atom[30]). The C_6B_4 systems can be characterized as dynamically stable, since the calculated phonon spectrum does not contain any appreciable imaginary modes (Figure 2).

To gain insight into the electronic properties of the C_6B_4 monolayers, we calculated the band structure and its density of states (DOS). As the calculations showed (Figure 3), the oc-*ex*-C_6B_4 system is a narrow-gap semiconductor with an indirect minimum junction from the valence band (point Y) to the conduction band (point Γ) with a band gap of 0.55 eV. The oc-*in*-C_6B_4 system can be characterized as a semimetal, that is, without a band gap and with an indirect minimal transition from the valence band (point Y) to the conduction band (point Γ).

The potential applicability of the predicted 2D sheets was explored based on the analysis of their mechanical properties. The necessary and sufficient Born criterion for the mechanical stability of a 2D crystal is determined by the relations $c_{11} > 0$, $c_{11}c_{22} > c_{12}^2$ and $c_{66} > 0$.[31] As listed in Table 2, the elastic constants of the monolayers meet the mechanical stability criterion, indicating that the predicted monolayers are mechanically stable. The C_6B_4 monolayers are anisotropic materials with two mutually orthogonal directions for which their characteristics differ.

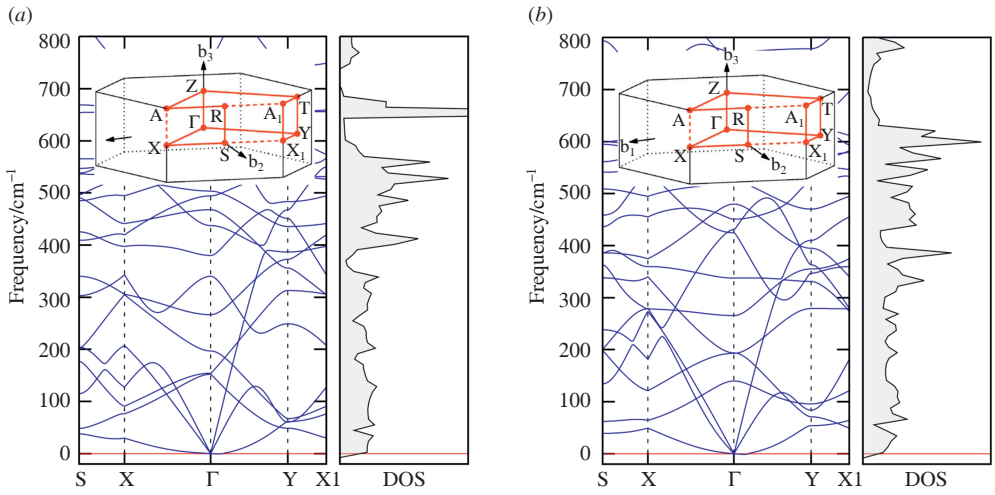

Figure 2 Calculated phonon dispersion curves along high-symmetry lines in the first Brillouin zone and phonon DOS for (*a*) oc-*ex*-C_6B_4 and (*b*) oc-*in*-C_6B_4.

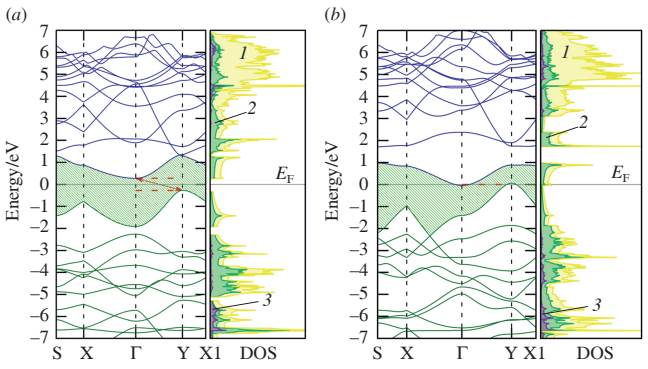

Figure 3 Calculated electronic band structure along high-symmetry lines in the first Brillouin zone and (*1*) total, (*2*) *p*-electron and (*3*) *s*-electron DOS for (*a*) oc-*ex*-C_6B_4 and (*b*) oc-*in*-C_6B_4.

The calculated values of Young's modulus are much higher along the *y*-axis (the direction of extended boron–carbon chains) than along the *x*-axis, which is due to the strong bonding within the chains, which increases the resistance to elastic deformation in this direction. These materials can be described as flexible and soft. The elastic characteristics of the C_6B_4 monolayers are close to those of theoretically designed phosphoborane[32] and arsaborane,[33] as well as experimentally studied MoS_2.[34] The systems under consideration are characterized by extremely high values of Poisson's ratio, reaching 1.5 (see Table 2), corresponding to the force applied along the direction of the interfragment chains. Although high Poisson's ratios are typical for systems containing chain substructures, the calculated values are significantly higher than those obtained for other 2D derivatives, such as systems with acetylene ($\nu_{max} = 0.4$–0.9)[35] or boron ($\nu_{max} = 0.7$)[31] chains.

In order to more clearly evaluate the changes in Young's modulus and Poisson's ratio relative to different directions, we constructed polar diagrams showing the corresponding dependences of these quantities on the polar angle θ (Figure 4). The polar diagrams clearly show that Young's modulus and Poisson's ratio exhibit a high degree of anisotropy. Both systems are characterized by high values of the mechanical anisotropy coefficient Y_y/Y_x, which are 6.61 and 4.16 for oc-*ex*-C_6B_4 and oc-*in*-C_6B_4, respectively. In the case of the oc-*ex*-C_6B_4 monolayer, the anisotropy coefficient significantly exceeds the parameters of 2D systems with the highest characteristics (4.9 for B_4S[31] or 2.5 for black phosphorus[36]). It is interesting to note that in the case of the oc-*ex*-C_6B_4 system, the Poisson's ratio takes negative values for directions forming angles with the O_x axis from 31° to 59°, reaching the lowest value of –0.28 at an angle of 49.5°. Thus, the oc-*ex*-C_6B_4 monolayer can be characterized as an anisotropic auxetic.

Based on building blocks **11a**,**b**, two isomeric crystal structures can also be formed (Figure 5). They have a base-centered orthorhombic Bravais crystal lattice, in which the primitive unit cell is based on eight carbon and four boron atoms with a stoichiometric ratio of 8 : 4 (C_8B_4). The introduction of additional >C–C< bridges between two diboracyclopentadiene

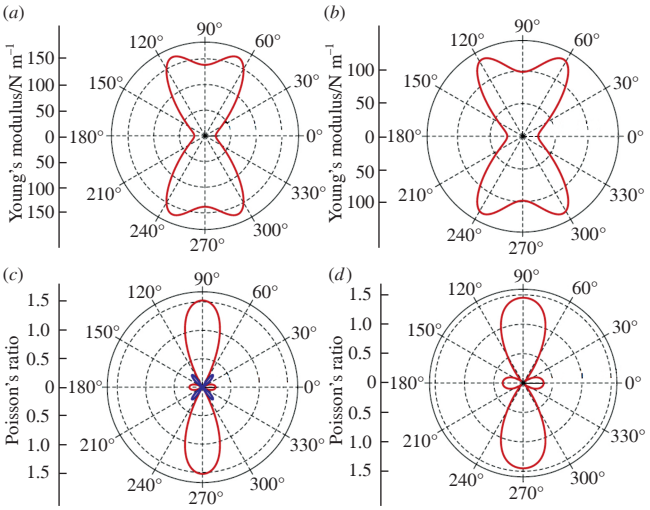

Figure 4 Directional dependence of (*a*),(*b*) Young's modulus and (*c*),(*d*) Poisson's ratio in (*a*),(*c*) oc-*ex*-C_6B_4 and (*b*),(*d*) oc-*in*-C_6B_4 monolayers. Blue lines correspond to negative values of Poisson's ratio.

Table 2 Calculated elasticity constants (c_{ij}/N m^{-1}), Young's modulus (Y_{2D}/N m^{-1}) and Poisson's ratio (ν) for 2D monolayers.

System	c_{11}	c_{12}	c_{22}	c_{66}	Y_x	Y_y	Y_y/Y_x	ν_x	ν_y
oc-*ex*-C_6B_4	32.24	49.15	213.20	50.25	20.91	138.28	6.61	0.23	1.52
oc-*in*-C_6B_4	48.00	69.63	199.52	39.46	23.71	98.54	4.16	0.35	1.45
oc-*ex*-C_8B_4	37.90	50.62	180.72	51.68	23.72	113.12	4.79	0.28	1.34
oc-*in*-C_8B_4	56.64	59.92	199.49	45.01	38.64	136.11	3.52	0.30	1.06

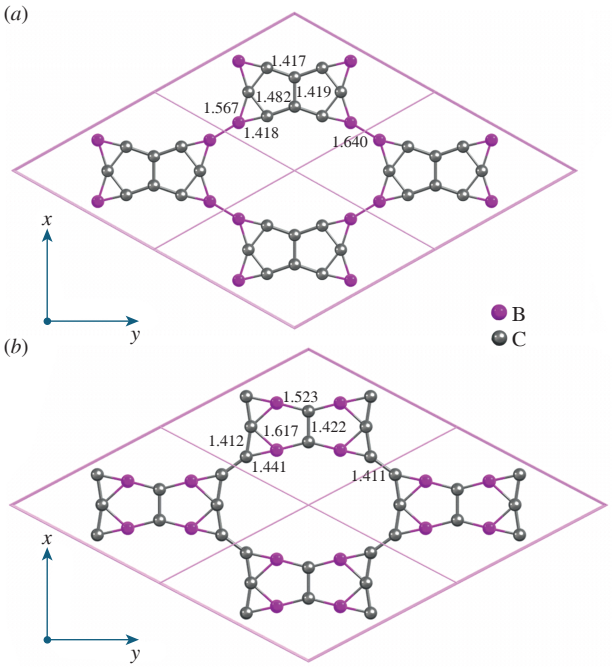

Figure 5 Geometric characteristics of (*a*) oc-*ex*-C_8B_4 and (*b*) oc-*in*-C_8B_4 2D crystals.

fragments inside the building block does not lead to any fundamental changes in the stability and properties of the 2D systems. The calculated cohesive energies for oc-*ex*-C_8B_4 and oc-*in*-C_8B_4 monolayers are slightly higher than those of the corresponding C_6B_4 analogs and amount to 6.82 and 6.90 eV per atom, respectively. The phonon spectra of both systems (Figure S1, see Online Supplementary Materials) do not contain any appreciable imaginary modes, confirming the kinetic stability of these derivatives.

At the same time, the introduction of additional >C–C< bridges is accompanied by a decrease in the conductive properties of the C_8B_4 derivatives compared to the C_6B_4 analogs. As in the pair of C_6B_4 systems, the oc-*in*-C_8B_4 isomer with internal continuous carbon rings is characterized by more pronounced conductive properties. The oc-*ex*-C_8B_4 monolayer is a wide-gap semiconductor with a direct transition from the valence band to the conduction band at the Y point, while the band gap is 2.03 eV. For the oc-*in*-C_8B_4 monolayer, the band gap is significantly smaller and equal to 0.68 eV, the minimum transition from the valence band to the conduction band is also direct at the Y point (Figure S2).

The C_8B_4 monolayers are also mechanically stable. The presence of additional perpendicular >C–C< bridges in the pair of C_8B_4 building blocks provides higher rigidity of the system compared to the pair of C_6B_4 analogs and leads to slightly lower values of the Poisson's ratio in the direction of extended chains and the mechanical anisotropy coefficient (Table 2 and Figure S3). Like the oc-*ex*-C_6B_4 system, the oc-*ex*-C_8B_4 system can be characterized as an anisotropic auxetic. The Poisson's ratio of the oc-*ex*-C_8B_4 crystal structure takes negative values for directions forming angles from 34° to 56° with the O_x axis, reaching the lowest value of –0.18 at an angle of 47.7°.

Thus, the calculations show that based on diboraspiropentadiene, various graphene-like 2D surfaces can be constructed, which include multiple non-classical ptC centers and characterized by structural and dynamic stability. A unique feature of such systems is the pronounced in-plane anisotropy of mechanical properties with high values of the mechanical anisotropy coefficient (up to 6.6) and maximum values of the Poisson's ratios (up to 1.5), significantly exceeding the characteristics of previously studied 2D systems. Isomers oc-*ex*-C_6B_4 and oc-*ex*-C_8B_4, containing a continuous six-membered carbon ring within the structural block, have negative Poisson's ratios for some directions and can be characterized as anisotropic auxetics. The presence of additional >C–C< bridges inside the C_8B_4 structural blocks leads to an increase in the rigidity of the systems, as well as to a decrease in their conductivity and mechanical anisotropy coefficient. Thus, modification of the structural blocks allows for targeted regulation of the characteristics of the resulting material.

This work was supported by the Russian Science Foundation (grant no. 23-23-00338).

Online Supplementary Materials

Supplementary data associated with this article can be found in the online version at doi: 10.71267/mencom.7595.

References

1 R. Hoffmann, R. W. Alder and C. F. Wilcox, Jr., *J. Am. Chem. Soc.*, 1970, **92**, 4992; https://doi.org/10.1021/ja00719a044.
2 V. I. Minkin, R. M. Minyaev and R. Hoffmann, *Russ. Chem. Rev.*, 2002, **71**, 869; https://doi.org/10.1070/RC2002v071n11ABEH000729.
3 P. von Ragué Schleyer and A. I. Boldyrev, *J. Chem. Soc., Chem. Commun.*, 1991, 1536; https://doi.org/10.1039/c39910001536.
4 L.-M. Yang, E. Ganz, Z. Chen, Z.-X. Wang and P. von Ragué Schleyer, *Angew. Chem., Int. Ed.*, 2015, **54**, 9468; https://doi.org/10.1002/anie.201410407.
5 R. M. Minyaev and V. I. Minkin, *Russ. J. Gen. Chem.*, 2008, **78**, 732; https://doi.org/10.1134/S1070363208040348.
6 T. N. Gribanova, R. M. Minyaev and V. I. Minkin, *Russ. J. Gen. Chem.*, 2005, **75**, 1651; https://doi.org/10.1007/s11176-005-0482-9.
7 V. I. Minkin, R. M. Minyaev, A. G. Starikov and T. N. Gribanova, *Russ. J. Org. Chem.*, 2005, **41**, 1289; https://doi.org/10.1007/s11178-005-0337-1.
8 R. M. Minyaev, T. N. Gribanova and V. I. Minkin, in *Comprehensive Inorganic Chemistry II: From Elements to Applications*, 2nd edn., eds. J. Reedijk and K. Poeppelmeier, Elsevier, Amsterdam, 2013, vol. 9, pp. 109–132; https://doi.org/10.1016/B978-0-08-097774-4.00904-9.
9 T. N. Gribanova, R. M. Minyaev and V. I. Minkin, *Russ. J. Gen. Chem.*, 2008, **78**, 750; https://doi.org/10.1134/S107036320804035X.
10 T. N. Gribanova, R. M. Minyaev and V. I. Minkin, *Russ. Chem. Bull.*, 2023, **72**, 2565; https://doi.org/10.1007/s11172-023-4060-2.
11 E. Jimenez-Izal, M. Saeys and A. N. Alexandrova, *J. Phys. Chem. C*, 2016, **120**, 21685; https://doi.org/10.1021/acs.jpcc.6b07612.
12 Y. Li, Y. Liao, P. von Ragué Schleyer and Z. Chen, *Nanoscale*, 2014, **6**, 10784; https://doi.org/10.1039/c4nr01972e.
13 P. D. Pancharatna, M. A. Méndez-Rojas, G. Merino, A. Vela and R. Hoffmann, *J. Am. Chem. Soc.*, 2004, **126**, 15309; https://doi.org/10.1021/ja046405r.
14 J. Dai, X. Wu, J. Yang and X. C. Zeng, *J. Phys. Chem. Lett.*, 2014, **5**, 2058; https://doi.org/10.1021/jz500674e.
15 A. Nandula, Q. T. Trinh, M. Saeys and A. N. Alexandrova, *Angew. Chem., Int. Ed.*, 2015, **54**, 5312; https://doi.org/10.1002/anie.201501049.
16 X. Wu, Y. Pei and X. C. Zeng, *Nano Lett.*, 2009, **9**, 1577; https://doi.org/10.1021/nl803758s.
17 Z. Zhang, X. Liu, B. I. Yakobson and W. Guo, *J. Am. Chem. Soc.*, 2012, **134**, 19326; https://doi.org/10.1021/ja308576g.
18 T. N. Gribanova, R. M. Minyaev and V. I. Minkin, *Collect. Czech. Chem. Commun.*, 1999, **64**, 1780; https://doi.org/10.1135/cccc19991780.
19 R. M. Minyaev and T. N. Gribanova, *Russ. Chem. Bull.*, 2000, **49**, 783; https://doi.org/10.1007/BF02494697.
20 R. M. Minyaev, T. N. Gribanova, V. I. Minkin, A. G. Starikov and R. Hoffmann, *J. Org. Chem.*, 2005, **70**, 6693; https://doi.org/10.1021/jo050651j.
21 W. Sun, C. Zhang and Z. Cao, *J. Phys. Chem. C*, 2008, **112**, 351; https://doi.org/10.1021/jp0771522.
22 C. Zhang, W. Sun and Z. Cao, *J. Am. Chem. Soc.*, 2008, **130**, 5638; https://doi.org/10.1021/ja800540x.
23 C. Zhang, P. Wang, J. Liang, W. Jia and Z. Cao, *J. Mol. Struct.: THEOCHEM*, 2010, **941**, 41; https://doi.org/10.1016/j.theochem.2009.10.036.

24 R. M. Minyaev, V. E. Avakyan, A. G. Starikov, T. N. Gribanova and V. I. Minkin, *Dokl. Chem.*, 2008, **419**, 101; https://doi.org/10.1134/S001250080804006X.
25 V. I. Minkin, V. E. Avakyan and R. M. Minyaev, *Russ. Chem. Bull.*, 2011, **60**, 2188; https://doi.org/10.1007/s11172-011-0337-y.
26 J. Emsley, *The Elements*, 2nd edn., Clarendon Press, Oxford, 1991; https://archive.org/details/elements0000emsl_j5r1/mode/2up.
27 A. Quandt, C. Özdoğan, J. Kunstmann and H. Fehske, *Nanotechnology*, 2008, **19**, 335707; https://doi.org/10.1088/0957-4484/19/33/335707.
28 D. V. Steglenko, S. A. Zaitsev, R. M. Minyaev and V. I. Minkin, *Russ. J. Inorg. Chem.*, 2019, **64**, 1031; https://doi.org/10.1134/S0036023619080163.
29 N. D. Drummond, V. Zólyomi and V. I. Fal'ko, *Phys. Rev. B: Condens. Matter Mater. Phys.*, 2012, **85**, 075423; https://doi.org/10.1103/PhysRevB.85.075423.
30 M. E. Dávila, L. Xian, S. Cahangirov, A. Rubio and G. Le Lay, *New J. Phys.*, 2014, **16**, 095002; https://doi.org/10.1088/1367-2630/16/9/095002.
31 D. V. Steglenko, T. N. Gribanova and R. M. Minyaev, *J. Phys. Chem. C*, 2023, **127**, 15533; https://doi.org/10.1021/acs.jpcc.3c02427.
32 D. V. Steglenko, N. V. Tkachenko, A. I. Boldyrev, R. M. Minyaev and V. I. Minkin, *J. Comput. Chem.*, 2020, **41**, 1456; https://doi.org/10.1002/jcc.26189.
33 N. Fedik, D. V. Steglenko, A. Muñoz-Castro, R. M. Minyaev and V. I. Minkin, *J. Phys. Chem. C*, 2021, **125**, 17280; https://doi.org/10.1021/acs.jpcc.1c02939.
34 S. Bertolazzi, J. Brivio and A. Kis, *ACS Nano*, 2011, **5**, 9703; https://doi.org/10.1021/nn203879f.
35 S. A. Hernandez and A. F. Fonseca, *Diamond Relat. Mater.*, 2017, **77**, 57; https://doi.org/10.1016/j.diamond.2017.06.002.
36 J.-W. Jiang and H. S. Park, *J. Phys. D: Appl. Phys.*, 2014, **47**, 385304; https://doi.org/10.1088/0022-3727/47/38/385304.

Received: 15th August 2024; Com. 24/7595